

Lactate monitoring in droplet microfluidics: a cautionary tale in assay miniaturisation

Received 00th January 20xx,
Accepted 00th January 20xx

Chi Leng Leong,^{a,b} Sharon Coleman,^a Adrian M Nightingale,^a Sammer-ul Hassan,^a David Voegeli,^c
Martyn G Boutelle^{b*} and Xize Niu^{a*}

DOI: 10.1039/x0xx00000x

www.rsc.org/

We present the development of a droplet-based device for real-time continuous lactate measurement, highlighting how protocols from long-established homogeneous enzymatic assays require careful re-optimisation before their migration into miniaturised droplet-based microfluidics.

Droplet microfluidics has become a valuable platform for high-throughput chemical reactions¹ and biological analysis.² Using immiscible carrier fluids and channel geometries, such as T-junctions or flow-focusing junctions, aqueous sample streams can be spontaneously broken up into discrete droplets. Encapsulating the sample in droplets removes the risk of contamination or evaporation,³ whilst also preserving the temporal resolution and concentration profile of the analyte.^{4,5} Recent developments have shown that nanolitre volumes can be sampled continuously and directly from human tissue, such as dermal tissue⁶ or internal organs,⁷ and be immediately analysed with biomarker-specific reagent in droplets, leading to 'wearable' chemical labs that could be used to monitor the fluctuation and metabolism of biomarkers and drug molecules *in vivo*.⁶ An apparent advantage in developing droplet microfluidic sensors is the availability of a wide range of well calibrated wet-chemical assays that are routinely used in research and clinical laboratories. The protocols of these wet-chemistry assays can be miniaturised into droplets by taking advantage of the various droplet manipulation techniques, such as generation (and mixing),⁸ merging,⁹ sorting,¹⁰ diluting,¹¹ splitting,¹² and analysis¹³ to produce data that is comparable with the golden standard methods suitable for diagnostics and clinical decision making.

Lactate is an important metabolic marker associated with insufficient tissue oxygenation/tissue ischaemia.¹⁴ The continuous monitoring of lactate is crucial in a variety of patho/physiological conditions such as free flap transplants¹⁵ and secondary brain injury,¹⁶ as well as in sport science.¹⁷ In these conditions, lactate can vary with a large dynamic range (from a baseline of approximately 1 mM to a maximum of 20 mM) within a short period of time (e.g. minutes).^{14,18} Current methods sample and analyse using electrochemical sensors.^{17,18} They operate solely in continuous flow, rely on an additional diffusional barrier to extend the sensing range,¹⁷ and are susceptible to surface fouling and sensitivity degradation over long-term use. Moreover Taylor dispersion smears the fidelity of chemical information entering the sensor system, fundamentally limiting the temporal resolution of continuous measurements.⁵ As such there is a need for microfluidic analysis methods that can preserve the temporal detail of chemical variations at the point of sampling to the point at which they are analysed. Here we report a solution-based lactate assay implemented in droplet flow that addresses this need and can be used in a droplet-based wearable sensor.⁶ However, the assay highlights the need to exercise caution as reaction volumes decreases to nanolitre or picolitre levels as direct downscaling can lead to problems previously unseen at benchtop volumes.

In developing a protocol for measuring lactate in droplet microfluidics, we first studied the feasibility of directly transferring a single-step homogeneous colorimetric lactate assay¹⁹ into a droplet microfluidic format. Traditional homogeneous enzymatic assays, such as those typically used to measure lactate, are optimised for sensitive spectrophotometers with long path lengths (~ 1 cm). They typically require dilution of samples by 10 to 100-fold and use low concentrations of enzymes so that pseudo-steady-state conditions apply.¹⁹ Such dilutions are difficult to achieve in microfluidics for point-of-care or real-time high throughput analysis. Furthermore, optical path lengths in microfluidic systems are typically less than a few hundred microns and the

^a Faculty of Engineering and Physical Sciences, University of Southampton, Southampton, U.K. SO17 1BJ

^b Department of Bioengineering, Imperial College London, South Kensington, London, U.K. SW7 2AZ

^c Faculty of Health Sciences, University of Southampton, Southampton, U.K. SO17 1BJ

*Corresponding authors. Emails: x.niu@soton.ac.uk; m.boutelle@imperial.ac.uk

detectors in point-of-care systems relatively crude. To counteract this we applied the maxim ‘nothing succeeds like excess’- increasing the final sample concentration by using lower dilutions and increasing the reagent concentration, hence delivering a stronger measured signal.

We began by characterising the assay in the bulk. The assay consisted of three components: lactate oxidase (LOx), horseradish peroxidase (HRP) and a mediator dye, 2,2'-azino-bis(3-ethylbenzothiazoline-6-sulfonic acid) diammonium salt (ABTS), premixed into a single reagent (60 U.mL⁻¹, 100 U.mL⁻¹, and 100 mM respectively in 0.1 M phosphate buffer, pH 7.0) and then added to the lactate samples. To simulate the online sampling and analysis conditions necessary for a point-of-care microfluidic system, the lactate sample was undiluted and a 1:1 ratio of sample to reagent was used. Optical measurement was performed in a 96-well plate using a commercial spectrometer (FLUOstar Omega; BMG LABTECH).

The reaction scheme is shown in Fig. 1(a). In the presence of oxygen (O₂), LOx converts lactate into pyruvate and produces hydrogen peroxide (H₂O₂) as a by-product. The H₂O₂ is then converted by HRP into water while it simultaneously oxidises

concentrations, below 1 mM, the conversion of O₂ to H₂O₂ occurs favourably, leading to a gradual build up in the concentration of the final product, ABTS⁺. However, as the lactate concentration increases, the rapid turnover of lactate by LOx depletes the O₂ supply (~250 μM of dissolved O₂ in solution²²). In the absence of O₂, the enzyme substitutes an oxidised mediator,²³ ABTS⁺, as an electron acceptor, which is reduced back to its colourless state, ABTS, allowing the enzyme to continue lactate consumption. Hence, two lactate molecules are consumed with no overall colour production, as shown in the futile mediation reaction scheme shown in Fig. 1(b). Shaking the mixture to add O₂ gave a temporary return of colour but this was followed by colour loss due to O₂ depletion (data not shown).

When transferring this reaction scheme into droplet microfluidics, two solutions were envisaged: (1) an inherent increase in O₂ supply and (2) potential temporospatial separation of the two enzymatic reaction steps. The material properties of the microfluidic system facilitate the former: The carrier oil, typically a perfluorinated oil such as FC-40 (Fluorinert, 3M), has a higher solubility for O₂ compared to water by 10-30 times,^{22, 24} and the most commonly used substrate material, PDMS, is also highly permeable to O₂.²² We found however that the increased O₂ concentrations associated with microfluidic systems were insufficient to remove futile mediation. Negligible colour was developed in droplets of reagent and sample (20 mM lactate, 1:1 reagent: sample ratio) generated at a T-junction (as shown for example in Supplementary Video 1). The second solution was to separate the LOx and HRP enzymatic reactions. This could be achieved by first forming isolated micro-droplets containing no ABTS/HRP and then dosing ABTS/HRP into the droplets once the LOx reaction has run to completion. Since there is no or very little lactate left, the coexistence of LOx and ABTS⁺ should not result in futile mediation.

A microfluidic chip to perform the assay in two distinct steps was subsequently designed and fabricated in PDMS. As shown in Fig. 2(a). In Step 1 LOx (60 U.mL⁻¹ in 0.1 M phosphate buffer) was added to the lactate sample stream at a volumetric ratio of 1:1, after which the aqueous stream was immediately broken up into discrete droplets at a T-junction, carried by an immiscible carrier oil (Fluorinert FC-40 with 0.4 % tri-block copolymer surfactant²⁵). The droplets then travelled through a serpentine channel with enough reaction time for the LOx reaction to run to completion. With the chip design used here, this reaction time could be varied between 30 and 90 s by controlling the total flow rate, however varying the channel length could have been used to potentially change the reaction time from less than a second to tens of minutes.” In Step 2, the droplets were dosed with HRP/ABTS (100 U.mL⁻¹, 100 mM respectively in 0.1 M phosphate buffer) at a second T-junction, triggering the conversion of the H₂O₂ (produced in Step 1) into H₂O and the oxidation of ABTS to ABTS⁺, resulting in an intense blue-green droplet stream. All reagents were purchased from Sigma Aldrich.

Liquid pumping and droplet generation was performed with our previously-described miniature peristaltic pump.⁶ In brief the

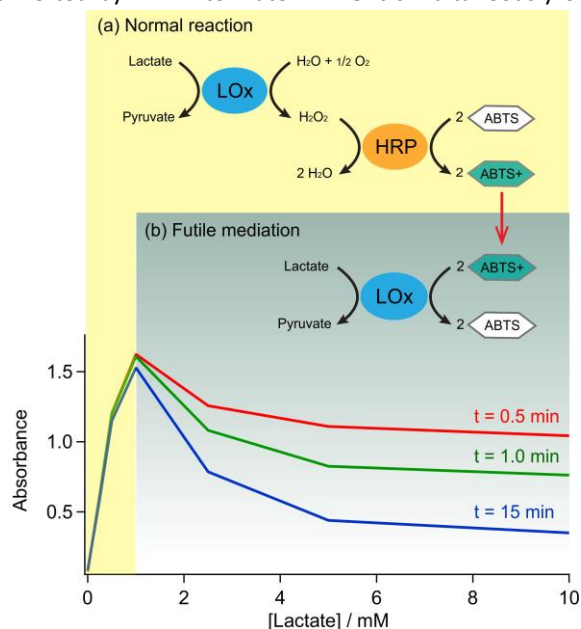


Fig. 1 Preliminary test of the one-step homogeneous solution-based enzymatic assay for lactate in a 96-well plate. (a) Up until 1 mM the response is dominated by normal reaction, with the measured absorbance resulting from the ABTS⁺ reaction product. (b) Above 1 mM lack of oxygen drives futile mediation, greatly reducing the measured response.

the colourless ABTS into ABTS⁺, which is blue-green in colour.¹⁹ The absorbance of ABTS⁺ is measured at 650 nm and the intensity corresponds to the concentration of lactate.²⁰ Figure 1 shows a fast (< 30 s) and stable colour development at low lactate concentrations, with a maximum absorbance at 1 mM. Above this concentration, an intense colour was initially observed but it quickly faded away and the mixture became colourless. The absorbance values dropped back below 1 mM, resulting in a non-unique analytical response curve.

A further study of the reaction parameters showed that this loss of colour at higher lactate concentrations is due to a phenomenon known as futile mediation.²¹ At low substrate

peristaltic pump, built in-house, drives up to 6 channels of oil and aqueous streams simultaneously with the oil and aqueous streams driven in anti-phase pulses into a T-junction chip. The pulsed oil and aqueous flows enter the T-junction alternately, resulting in a “chopping”-like method of droplet generation.²⁶ This droplet generation strategy guarantees the droplet volumes are solely determined by the pump design and are insensitive to liquid properties and flow rates.⁶

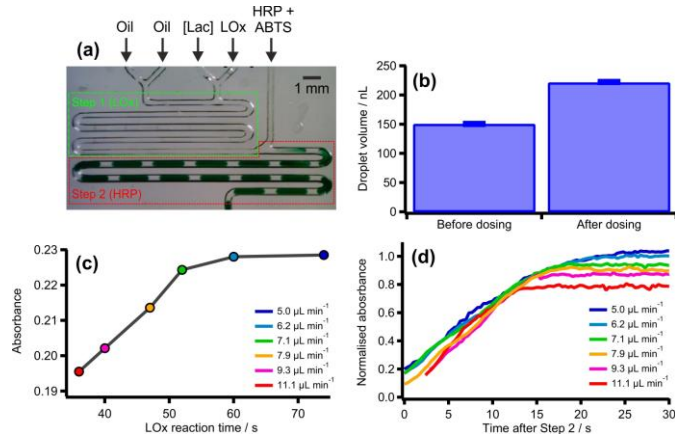


Fig. 2 Droplet microfluidic approach for a two-step enzymatic reaction demonstrating precise and full control for reaction optimisation. a) Image of microfluidic chip, highlighting the two reaction steps. Transparent droplets containing lactate samples and LOx at a 1:1 ratio are generated at the T-junction in Step 1. They then travel through the serpentine with enough time for the LOx reaction to run to completion. Upon dosing with HRP/ABTS at the second T-junction in Step 2, an intense blue-green colour starts to develop. b) Droplet volumes before and after dosing, with error bars showing the standard deviation. c) Droplet absorbance with different flow rates, showing the effect of different residence times for Step 1. d) Droplet absorbance as a function of time after the dosing step that begins Step 2

Uniform size droplet generation and accurate reagent addition into the pre-formed droplets has not been a trivial task in droplet microfluidics. Reagent addition into pre-formed droplets has previously been achieved by merging pairs of droplets,⁹ using a picoinjector,²⁷ or direct-injection in three-phase flow.²⁸ Here we used the simpler direct-injection method due to the predefined flow provided by our peristaltic pump, which introduces liquid in a controlled pulses without any ramp-up time or drift.⁶ This meant that we could be sure that a droplet would consistently be positioned at the second T-junction only when the HRP reagent pulse was introduced. We quantified the droplet volume before and after dosing by substituting the colourless aqueous streams with solutions containing food dye. The total flow rate was set to $9.3 \mu\text{L min}^{-1}$ and the droplet generation rate was 0.33 Hz. Fig. 2(b) shows that the volume of droplets in Step 1 and after dosing (Step 2) was $149.5 \pm 0.8 \text{ nL}$ and $220.6 \pm 1.0 \text{ nL}$ ($n = 250$ for both populations), respectively with a relative standard deviation less than 1 % in each case indicating monodisperse droplet populations. Such a small size variation is important for ensuring reproducible reaction stoichiometry and hence the precision of the final analysis.

The reaction in Step 1 was first investigated to ascertain the time required to go to completion. For a fixed LOx concentration, the reaction time increases with increasing substrate concentration. A lactate concentration of 20 mM was

chosen as it represents a very high physiological concentration and the maximum anticipated reaction time. As the distance between the T-junctions at Step 1 (droplet generation) and Step 2 (reagent dosing) is fixed, the reaction time is therefore inversely related to the flow rate. Hence, a faster flow rate gives a shorter travel time between T-junctions. If the reaction time is too short for complete lactate conversion, this will lead to the co-existence of unreacted lactate, LOx and ABTS^+ at Step 2, resulting in futile mediation. Since the Step 1 reaction is colourless, we also implemented Step 2 by dosing the second reagent into the droplets and then measured the colour (absorbance) of the droplets downstream of the chip using an in-house built flow cell with a path length of approximately 0.5 mm.²⁹ The flow cell was composed of an LED (637 nm, Avago Technologies) and light-to-voltage converter (TSL257, Texas Advanced Optoelectronic Solutions) positioned either side of PTFE tubing. All components were held within a black acrylic body, which had been micromachined such that the light from the LED travelled through the centre of the tubing to the light-to-voltage converter with a clearly defined 0.4 mm-wide light path. The flow cell was sufficiently far downstream that the Step 2 reaction had reached completion irrespective of the flow rate. Fig. 2(c) shows that the droplet absorbance increased with reaction time and plateaued after 60 s (total flow rate $6.2 \mu\text{L min}^{-1}$) at room temperature (20°C). Therefore, 60 s was deemed sufficient for the reaction in Step 1 to have gone to completion. Note that for a lactate concentration lower than 20 mM, a higher flow rate could be used as the reaction would reach completion quicker.

For calibration of Step 2, the microfluidic device was run using the same high concentration of lactate (20 mM). Colour generation was tracked by analysing videos of the droplets travelling through the chip, with absorbance values calculated using the light transmission through the droplets in Step 1 as a blank measurement. Fig. 2(d) shows the colour development at different flow rates after dosing. Time zero was defined as when the droplet was dosed with HRP/ABTS. Droplet absorbance increased monotonically with full colour development occurring at 25 s post-dosing at a total flow rate of $5 \mu\text{L min}^{-1}$, as indicated by the plateau response shown by the blue trace in Fig. 2(e). The different saturation levels after 25 s of reaction are proportional to the final concentration of H_2O_2 in the droplet. Importantly, this shows that by choosing the correct flow rates ($< 6.2 \mu\text{L min}^{-1}$) we can ensure that each reaction successfully completes without the risk of futile mediation.

To demonstrate that the two-step approach eliminates futile mediation, the equivalent one-step homogeneous assay was also performed with the same microfluidic chip. LOx and HRP/ABTS were both flowed into the first T-junction (in the same concentration ratio as for the two-step approach) and mixed with lactate before being broken up into discrete droplets. The dosing path of the second T-junction was blocked. The absorbance was measured downstream of the chip using the same detector used for the Step 1 optimisation and is shown by the black trace and triangular markers in Fig. 3(a). At low lactate concentrations ($< 0.5 \text{ mM}$), the one-step reaction gives a similar colour change to the two-step format (Fig. 3(a) blue

trace and circular markers). However, the absorbance for the one-step reaction decreases above this concentration, similar to the behaviour seen in the bulk (Fig. 1) demonstrating that futile mediation persists in droplet format. In contrast, when performed in two steps the droplet absorbance continued to rise with lactate concentration giving vividly coloured droplets (see Fig. 3(b) and Supplementary Video 2). Here the response goes off-linear above 3 mM as a result of deviations from the Beer-Lambert law at higher absorbance values. This effect can be reduced using a shorter path length, and we note that we have previously shown that with a suitable flow cell this setup can measure the full physiological range from limit of detection to 20 mM.⁶ Nonetheless, the strong colour development seen in the two-step procedure is in stark contrast with the transparent droplets seen for the single step setup (shown in Fig. 3(c) and Supplementary Video 1)."

With the reactions in these two steps understood, we then implemented the optimised assay into a wearable sensor which could sample and measure interstitial fluid. This system, described elsewhere,⁶ integrated peristaltic pump, optical flow cell, reagent and oil reservoirs, control electronics, and Bluetooth transmitter, into a small wearable device. It could continuously monitor glucose or lactate within interstitial fluid sampled using a subcutaneous microdialysis probe. There we

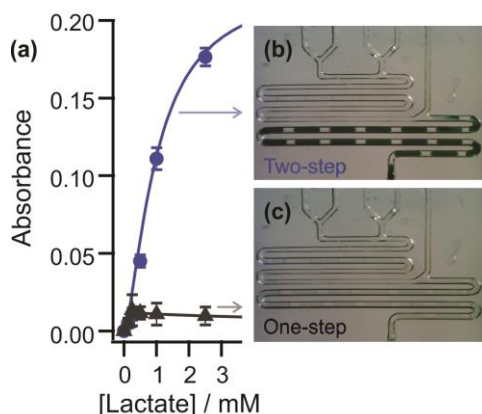


Fig. 3 a) Droplet absorbance for the lactate assay performed in one-step (triangle markers) and two-steps (circular markers). Error bars relate to standard deviation of the measurements. Colour development is much stronger in the two-step regime, as illustrated in representative images of a 20 mM lactate concentration flowing through the chip in two-step (b) and one step operation (c).

found that with appropriate flow cell changes, it could measure lactate over the physiological range, using the total flow rate of $5 \mu\text{L min}^{-1}$ established here, and had a limit of detection (quantified using the 3-sigma method³⁰) of 0.16 mM ($n = 3$)⁶. It was tested on healthy volunteers and successfully tracked small (5-25 %) changes in dermal tissue lactate caused by mild tissue ischaemia.

In conclusion, a droplet microfluidic system has been developed that uses a two-step homogenous enzymatic assay to quantify lactate concentrations *via* colourimetry. This system of two-step reactions can be extended for measurement of other molecules that are traditionally analysed in multiple steps or require incubation times between reaction steps. It can be implemented in wearable droplet microfluidic-based sensors⁶

to continuously sample and measure from a nanolitre droplet stream, providing highly-resolved real-time tracking of biomarkers, such as lactate, especially desirable in critical care monitoring applications.³¹ Moreover, this study highlights the potential risks in the miniaturisation of well-established benchtop assays into microfluidic formats, and the need to carefully adapt them. Here futile mediation was encountered but effectively eliminated by temporospatial separation of the reaction into two discrete reaction steps.

We thank the Engineering and Physical Sciences Research Council UK (EP/M012425/1) and Natural Environment Research Council UK (NE/P004016/1) for the funding of this research.

Notes and references

1. H. Song, D. L. Chen and R. F. Ismagilov, *Angewandte Chemie International Edition*, 2006, **45**, 7336-7356.
2. A. B. Theberge, F. Courtois, Y. Schaerli, M. Fischlechner, C. Abell, F. Hollfelder and W. T. S. Huck, *Angewandte Chemie International Edition*, 2010, **49**, 5846-5868.
3. X. Z. Niu, B. Zhang, R. T. Marszalek, O. Ces, J. B. Edel, D. R. Klug and A. J. deMello, *Chemical Communications*, 2009, 6159-6161.
4. M. Wang, G. T. Roman, K. Schultz, C. Jennings and R. T. Kennedy, *Analytical Chemistry*, 2008, **80**, 5607-5615.
5. S. Feng, E. Shirani and D. W. Inglis, *Biosensors*, 2019, **9**, 80.
6. A. M. Nightingale, C. L. Leong, R. A. Burnish, S.-u. Hassan, Y. Zhang, G. F. Clough, M. G. Boutelle, D. Voegeli and X. Niu, *Nature Communications*, 2019, **10**, 2741.
7. R. T. Kennedy, *Current Opinion in Chemical Biology*, 2013, **17**, 860-867.
8. P. Zhu and L. Wang, *Lab on a Chip*, 2017, **17**, 34-75.
9. X. Niu, S. Gulati, J. B. Edel and A. J. deMello, *Lab on a Chip*, 2008, **8**, 1837-1841.
10. Y. C. Tan, J. S. Fisher, A. I. Lee, V. Cristini and A. P. Lee, *Lab on a Chip*, 2004, **4**, 292-298.
11. X. Niu, F. Gielen, J. B. Edel and A. J. deMello, *Nat Chem*, 2011, **3**, 437-442.
12. D. R. Link, S. L. Anna, D. A. Weitz and H. A. Stone, *Physical Review Letters*, 2004, **92**, 054503.
13. E. Y. Basova and F. Foret, *Analyst*, 2015, **140**, 22-38.
14. G. A. Dienel, *Journal of Cerebral Blood Flow & Metabolism*, 2014, **34**, 1736-1748.
15. M. L. Rogers, P. A. Brennan, C. L. Leong, S. A. N. Gowers, T. Aldridge, T. K. Mellor and M. G. Boutelle, *Analytical and Bioanalytical Chemistry*, 2013, **405**, 3881-3888.
16. M. L. Rogers, D. Feuerstein, C. L. Leong, M. Takagaki, X. Niu, R. Graf and M. G. Boutelle, *ACS Chemical Neuroscience*, 2013, **4**, 799-807.
17. S. A. N. Gowers, V. F. Curto, C. A. Seneci, C. Wang, S. Anastasova, P. Vadgama, G.-Z. Yang and M. G. Boutelle, *Analytical Chemistry*, 2015, **87**, 7763-7770.
18. W. Jia, A. J. Bandodkar, G. Valdés-Ramírez, J. R. Windmiller, Z. Yang, J. Ramírez, G. Chan and J. Wang, *Analytical Chemistry*, 2013, **85**, 6553-6560.
19. R. E. Childs and W. G. Bardsley, *Biochemical Journal*, 1975, **145**, 93.
20. A. Llobera, V. J. Cadarso, M. Darder, C. Dominguez and C. Fernandez-Sanchez, *Lab on a Chip*, 2008, **8**, 1185-1190.

Journal Name

21. D. G. Georganopoulou, R. Carley, D. A. Jones and M. G. Boutelle, *Faraday Discussions*, 2000, **116**, 291-303.
22. P. Abbyad, P.-L. Tharaux, J.-L. Martin, C. N. Baroud and A. Alexandrou, *Lab on a Chip*, 2010, **10**, 2505-2512.
23. A. E. G. Cass, G. Davis, G. D. Francis, H. A. O. Hill, W. J. Aston, I. J. Higgins, E. V. Plotkin, L. D. L. Scott and A. P. F. Turner, *Analytical Chemistry*, 1984, **56**, 667-671.
24. J. Wang and F. Lu, *Journal of the American Chemical Society*, 1998, **120**, 1048-1050.
25. V. Chokkalingam, J. Tel, F. Wimmers, X. Liu, S. Semenov, J. Thiele, C. G. Figdor and W. T. S. Huck, *Lab on a Chip*, 2013, **13**, 4740-4744.
26. A. Nightingale, G. W. H. Evans, P. Xu, B. J. Kim, S.-u. Hassan and X. Niu, *Lab on a Chip*, 2017.
27. A. R. Abate, T. Hung, P. Mary, J. J. Agresti and D. A. Weitz, *Proceedings of the National Academy of Sciences*, 2010, **107**, 19163-19166.
28. A. M. Nightingale, T. W. Phillips, J. H. Bannock and J. C. de Mello, *Nature Communications*, 2014, **5**, 3777.
29. S. Hassan, A. M. Nightingale and X. Niu, *Analyst*, 2016, **141**, 3266-3273.
30. H.-P. Looock and P. D. Wentzell, *Sensors and Actuators B: Chemical*, 2012, **173**, 157-163.
31. J. Bakker, M. W. N. Nijsten and T. C. Jansen, *Annals of Intensive Care*, 2013, **3**, 12.